Photon Factory Activity Report 2024 #42 (2025)

BL-13A/2023G531

Changes in Electronic Structures of $Gd_{65}Co_{35}$ Metallic Glass by Cryogenic Rejuvenation

Shinya HOSOKAWA,[1,2,*] Hitoshi SATO,[3] Yasuhisa TEZUKA,[4] Jun-ichi ADACHI,[5] Kentaro KOBAYASHI,[1] Koji OHARA,[1] Tetsu ICHITSUBO,[6] Rui YAMADA,[6] and Hidemi KATO[6]
[1] Faculty of Materials for Energy, Shimane University, Matsue 690-8504, Japan
[2] Institute of Industrial Nanomaterials, Kumamoto University, Kumamoto 860-8555, Japan
[3] Hiroshima Research Institute for Synchrotron Radiation Science, Hiroshima University, Higashihiroshima 739-0046, Japan
[4] Graduate School of Science and Technology, Hirosaki University, Hirosaki 036-8561, Japan
[5] Photon Factory, Institute of Materials Structure Science, High Energy Accelerator Research Organization, Tsukuba, 305-0801, Japan
[2] Institute for Materials Research, Tohoku University, Sendai 980-8577, Japan

To experimentally clarify the changes in electronic structures of $Gd_{65}Co_{35}$ metallic glass (MG) by rejuvenation with temperature cycling (cryogenic rejuvenation), soft X-ray absorption and emission spectroscopies (SXAS and SXES) experiments were carried out at the Photon Factory in High Energy Accelerator Research Organization (PF-KEK) in addition to photoemission and inverse-photoemission spectroscopies (PES and IPES) experiments at Hiroshima University. By combining these techniques, element- and quantum number-selective partial density of states (pDOS) can be evaluated. By 40 repetitions of temperature changes between liquid N_2 and room temperatures, the Co 3*d* pDOSs are largely changed in magnitude. On the other hand, the Gd 4*d* and 4*f* pDOSs do not change beyond the range of experimental errors. These results are consistent with the structural changes by cryogenic rejuvenation found recently.

1 Introduction

Rejuvenation in glasses is generally defined as an excitation to a higher energy state by an external stress, opposite to the usual relaxation process by thermal annealing. A rejuvenation effect by temperature cycling in metallic glasses (MGs) was reported by Ketov et al. [1], which is caused by an internal stress with an external stimulation. According to their interpretation, if a glass is elastically heterogeneous, the thermal expansion coefficient has a distribution over the glass. Repeated temperature changes produce different magnitudes of thermal expansion in a glass, inducing shearing forces and resulting in a rejuvenation effect occurring in the glass. The validity of this simple picture is the subject of intensive debate.

Hufnagel, who named this phenomenon ‘cryogenic rejuvenation’, reviewed the rejuvenation effect of thermal cycling and suggested that such non-affine deformation must be appeared on an atomistic length scale [2]. The extent of the heterogeneity in glasses can be determined from the so-called β-relaxation peak in dynamic mechanical analysis (DMA) spectra [3]. Yamazaki measured DMA spectra on $Gd_{100-x}Co_x$ glasses [4], and a distinct β-relaxation peak was observed in the $Gd_{65}Co_{35}$ glass, in which the largest heterogeneity was expected.

We have carried out high energy X-ray diffraction (HEXRD) and anomalous X-ray scattering (AXS) experiments to experimentally clarify the structural changes, including partial atomic arrangements by cryogenic rejuvenation [5]. We observed clear structural changes in the nearest-neighbor range and partial atomic movements of Co from the first- to second-nearest neighbor shells. A distinct change was also detected in the microscopic elastic property by inelastic X-ray scattering (IXS), i.e., the width of longitudinal acoustic excitations broadens by about 20%, indicating an increase in the elastic heterogeneity of this MG.

Structural changes in $Gd_{65}Co_{35}$ MG by cryogenic rejuvenation should affect the electronic structures. We have investigated the changes in electronic structures by photoemission and inverse-photoemission spectroscopies (PES and IPES) as well as soft X-ray absorption and emission spectroscopies (SXAS and SXES). The information about the valence-band density of states (DOS) can be mainly obtained by PES and SXES, and that about the conduction-band DOS by IPES and SXAS. Note that these techniques have selective functions of the elements and electron quantum numbers. In this report, we describe the principles of the above electron spectroscopies, briefly give the experimental procedures, show the present results, discuss them, and finally summarize the present achievements.

2 Experiment

PES is well-known as a technique for evaluating valence-band DOS using the photoelectron effect. The quantum-number-selective function of the PES technique can be estimated by taking the incident photon energy dependence of photoionization cross-sections of the constituent elements into account. IPES is a technique to obtain conduction-band DOS. When a material is irradiated by an electron with a kinetic energy, the electron enters a conduction-band state of the material with the corresponding energy. This electron can radiatively lose its energy by releasing it to a conduction-band state with a lower energy, and emits a photon with the corresponding energy. The PES and IPES experiments were carried out at Hiroshima Research Institute for Synchrotron Radiation Science, Hiroshima University.

The above methods handle electrons in the measurement processes, and thus, a clean surface of the material is important to obtain the DOS correctly. In contrast, SXAS and SXES handle only photons for measurements, and thus, the surface cleanliness is relatively insensitive for the quality of the results.

For the present materials, for example, when a material is irradiated by a photon having an energy beyond the Co 2*p* absorption edge energy, the Co 2*p* electron is excited to the conduction band. Because of the selection rule of optical transition, the quantum number of the final state should be added or subtracted by one. In the present case, only Co 3*d* is the final state. Various methods for measuring the photon intensity can be applied to obtain the Co 3*d* conduction-band pDOS.

The SXES process is as follows. When an Co 2*p* electron is excited, a hole is generated at a core level. Then, an electron in the valence band with the Co 3*d* state undergoes a radioactive recombination with the hole and emits a photon with the corresponding energy. Hence, one can estimate the valence-band Co 3*d* pDOS by measuring the energy and intensity of the photons emitted from the material.

The SXES spectra were measured at BL13A of the PF-KEK using a Rowland-type monochromator with a spherical grating with a radius of 5 m and a line density of 1200 lines/mm and a photon detector with a CsI-coated multichannel plate. The energy resolution of SXES was about 0.3 eV FWHM. Details of the experimental setups are given elsewhere [6]. The SXES spectra of Co 3*d* valence-band pDOS were obtained with incident photon energies of 760-785 eV beyond the Co 2*p* absorption edge.

3 Results and Discussion

Figure 1(a) shows valence-band PES spectra of Gd$_{65}$Co$_{35}$ MG obtained at hv of 40-230 eV before (blue) and after (red) thermal treatment. As seen in the figure, the spectra in the range $hv \geq 80$ eV are mostly the same between the spectra before and after cryogenic rejuvenation. On the other hand, the spectra in the range $hv \leq 60$ eV after rejuvenation are smaller in magnitude at about E = -5 eV than those before the rejuvenation.

Such spectral changes can be easily understood by taking the hv dependence of photoionization cross-sections (σ_P) into account as shown in Fig. 1(b) [7]. The intensities of PES spectra depend strongly on the hv value through σ_Ps. The σ_P value of Co 3*d* electrons has a maximum at $hv \sim 50$ eV, while those of the other elements and quantum numbers are very small even when the Gd 4*f* electrons have only a small value of about 20% of Co 3*d* electrons. With increasing hv, σ_P of Co 3*d* largely decreases, while that of Gd 4*f* rapidly increases and becomes larger than that of Co 3*d* at $hv \sim 100$ eV. Accordingly, it can be concluded that the decrease in the PES spectra at about E = -5 eV by cryogenic rejuvenation is caused by the decrease in Co 3*d* pDOS in this energy region. Since Gd 4*f* electrons dominate the PES spectra at $hv > 100$ eV, Gd 4*f* pDOS in the valence band remain mostly unchanged by the cryogenic rejuvenation.

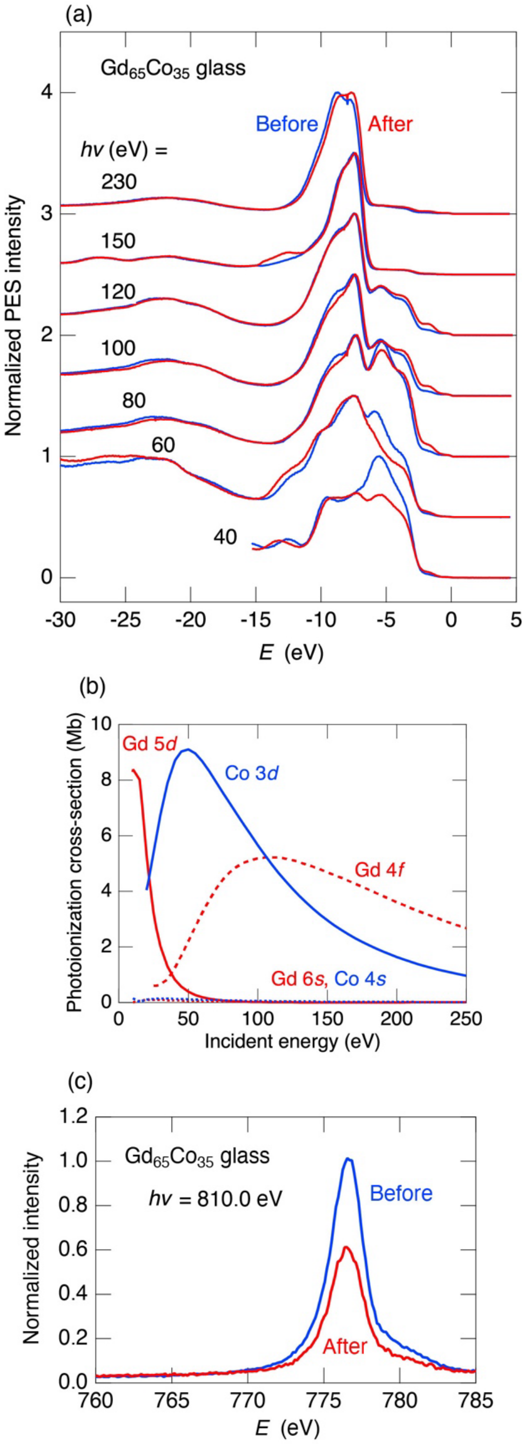

Fig. 1: Valence-band (a) PES spectra of Gd$_{65}$Co$_{35}$ MG before (blue) and after (red) thermal treatment. (b) Incident photon energy dependence of σ_P of the Gd- and Co-related electrons [7]. (c) Co 3*d* SXES spectra, where E_F is located at about 782 eV.

This result is confirmed by the spectral change in the SXES spectra shown in Fig. 1(c). The obtained spectra are only composed of the Co 3*d* pDOS when the spectra are generated by the Co 2*p*-3*d* excitations. The peak intensity considerably decreases by cryogenic rejuvenation. Since the peak position is about 5 eV below E_F, which is in excellent agreement with the changes in the PES spectra shown in Fig. 1(a). As a result, it can be concluded that only the Co 3*d* pDOS decreases by cryogenic rejuvenation in the valence-band DOS.

Concerning the conduction-band DOS, Fig. 2(a) shows the IPES spectra of $Gd_{65}Co_{35}$ MG before (blue) and after (red) temperature cycling. The spectra are composed of two peaks, and only the low energy peak at about 6.5 eV shifts towards lower energy by about 1.0 eV together with a sharpening of the peak feature. Since the incident electron energy of IPES was set to 50 eV and it is believed that the electron–photon relations in the PES and IPES processes are basically similar to each other, the obtained spectral changes originate from the Co 3*d* electrons.

This speculation can be confirmed by the changes in the Co 2*p*-3*d* SXAS spectra, as shown in Fig. 2(b). Because of the selection rule in the optical transitions, the Co 2*p* electrons are mainly excited to the Co 3*d* state by photons with an appropriate energy. As seen in the figure, the spectrum shifts towards lower energy by about 1 eV. The peak heights were normalized to the intensities of each peak, and thus, the peak magnitudes cannot be directly compared with each other. Nevertheless, the spectra of both IPES and SXAS exhibit similar shifts of the Co 3*d* states in the conduction band.

For the electrons related to Gd, Fig. 3 shows the Gd (a) 4*p*-4*d* (~265 eV) and (b) 4*d*-4*f* (~145 eV) SXAS spectra measured before (blue) and after (red) cryogenic rejuvenation. As seen in (a), the spectral features between the two spectra look slightly changed in magnitude, while the peak and shoulder positions in the spectra do not change beyond the range of error. Accordingly, the changes may originate from the experimental backgrounds of the SXAS measurements. In (b), the two spectra are almost identical. As a result, it can be concluded that no reliable differences were observed in the Gd-related SXAS spectra measured before and after cryogenic rejuvenation.

In summary, we measured the electron DOS of $Gd_{65}Co_{35}$ MG by four different techniques with to investigate the changes in pDOSs by cryogenic rejuvenation. The changes are observed in the Co 3*d* pDOS in both the valence and conduction bands by cryogenic rejuvenation. These changes are consistent with the structural changes around the Co atoms recently revealed by HEXRD and AXS measurements [5]. No clear changes were found in the Gd pDOSs, reflecting that the structural changes in the Gd atomic configurations in the glass were tiny. A MD simulation would be helpful in confirming the changes in the electronic structures; however, the existing MD simulation did not encompass the electronic structures of MGs. Thus, a further theoretical attempt is necessary to gain a detailed understanding of the cryogenic rejuvenation phenomena in MGs.

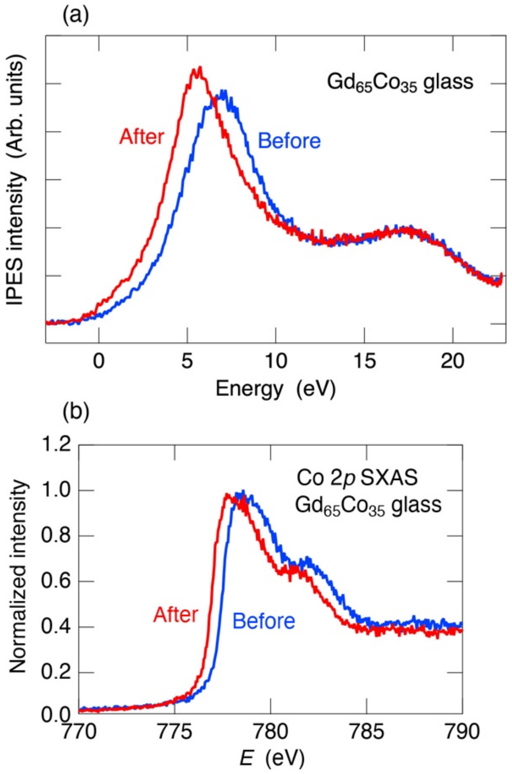

Fig. 2: Conduction-band (a) IPES and (b) Co 2*p* SXAS spectra of $Gd_{65}Co_{35}$ MG before (blue) and after (red) thermal treatment. In (b), E_F is located at about 772 eV.

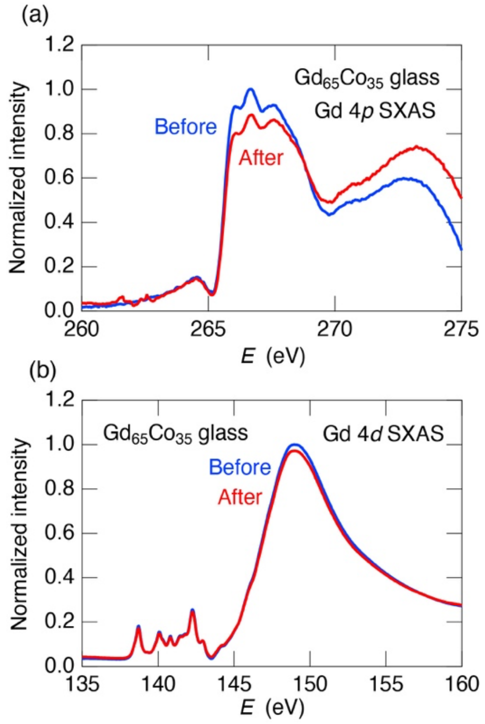

Fig. 3: Gd (a) 4*p*-4*d* and (b) 4*d*-4*f* SXAS spectra of $Gd_{65}Co_{35}$ MG before (blue) and after (red) thermal treatment.

Acknowledgement

PES and IPES experiments were performed at the HSRC (Nos. 21AU001, 21AU007, 20AG023, and 20AG024). SXAS and SXES experiments were conducted at BL13A of the PF-KEK (No. 2023G531). This work was performed under the GIMRT Program of the Institute for Materials Research, Tohoku University (Nos. 202312-CRKEQ-0027 and 202312-RDKGE-0038). These works were supported by the Japan Society for the Promotion of Science (JSPS) Grants-in-Aid for Transformative Research Areas (A) 'Hyper-Ordered Structures Science' (Nos. 21H05569 and 23H04117) and that for Scientific Research (C) (No. 22K12662), and by the Japan Science and Technology Agency (JST) CREST (No. JP-MJCR1861).

References

[1] S. V. Ketov *et al.*, *Nature* **524**, 200 (2015).
[2] T. C. Hufnagel, *Nat. Mater*. **14**, 867 (2015).
[3] G. P. Johari, *J. Non-Cryst. Solids* **307-310**, 317 (2002).
[4] Y. Yamazaki, Doctoral thesis (Tohoku University, 2016).
[5] S. Hosokawa *et al., Acta Mater.* **284**, 120616 (2025).
[6] S. Shin *et al.*, *Rev. Sci. Instrum*. **66**, 1584 (1995).
[7] J. J. Yeh and I. Lindau, *At. Data Nucl. Data Tables* **32**, 1 (1985).

* s_hosokawa@mat.shimane-u.ac.jp